frontiers in Chemistry

ORIGINAL RESEARCH
published: 08 May 2020
doi: 10.3389/fchem.2020.00325

Bi_2O_3 Nanoparticles Decorated Carbon Nanotube: An Effective Nanoelectrode for Enhanced Electrocatalytic 4-Nitrophenol Reduction

*Raviraj P. Dighole, Ajay V. Munde, Balaji B. Mulik and Bhaskar R. Sathe**

Department of Chemistry, Dr. Babasaheb Ambedkar Marathwada University Aurangabad, Aurangabad, India

4-Nitrophenol (4-NP) is present in most industrial waste water resources as an organic pollutant, and is a highly toxic and environmentally hazardous pollutant. Herein, we report that bismuth oxide (Bi_2O_3) decorated multi-walled carbon nanotubes (Bi_2O_3@MWCNTs) are the most prominent electrocatalyst for 4-NP electroreduction in acidic conditions. The electrocatalyst is synthesized by a simple chemical reduction method using ethylene glycol as a capping agent. The synthesized Bi_2O_3@MWCNTs electrocatalyst has been well-characterized by Fourier-transform infrared (FT-IR) spectroscopy, transmission electron microscopy (TEM), X-ray diffraction (XRD), and Raman spectroscopy. Bi_2O_3@MWCNTs have a cubic structure which is confirmed by XRD. TEM imaging reveals Bi_2O_3 NPs are ∼2 nm in size, are grown on MWCNTs and that these nanoparticles are active toward 4-NP electroreduction. The electrochemical studies by cyclic voltammetry measurements show that the Bi_2O_3@MWCNTs electrocatalyst can sense 4-NP at a very low potential i.e., −0.17 vs. saturated calomel electrode (SCE). Furthermore, electroanalytical parameters like scan rate and concentration dependence were studied with electrochemcial impedance spectroscopy (EIS) and the effect of pH on cathodic current was examined under experimental conditions. The lower limit of detection (LOD) was found to be 0.1 μM for the Bi_2O_3@MWCNTs nanomaterial and is excellent toward 4-NP. The present study has applications for reducing water pollution and for sorting out related issues.

Keywords: 4-NP, synergetic effect, Bi_2O_3@MWCNTs nanocomposite, environmental pollutant, electrochemistry

OPEN ACCESS

Edited by:
Vito Di Noto,
University of Padova, Italy

Reviewed by:
Tianyi Ma,
University of Newcastle, Australia
Mark D. Symes,
University of Glasgow,
United Kingdom

****Correspondence:***
Bhaskar R. Sathe
bhaskarsathe@gmail.com

Specialty section:
This article was submitted to Electrochemistry, a section of the journal Frontiers in Chemistry

Received: *09 January 2020*
Accepted: *30 March 2020*
Published: *08 May 2020*

Citation:
Dighole RP, Munde AV, Mulik BB and Sathe BR (2020) Bi_2O_3 Nanoparticles Decorated Carbon Nanotube: An Effective Nanoelectrode for Enhanced Electrocatalytic 4-Nitrophenol Reduction. Front. Chem. 8:325. doi: 10.3389/fchem.2020.00325

INTRODUCTION

4-Nitrophenol (4-NP) is an important compound as it is a precursor in the manufacturing processes of drugs, pesticides, dyes, fungicides, insecticides, explosives, and is used to darken leather (Li et al., 2012; Veerakumar et al., 2015; Rajkumar et al., 2018; Wu et al., 2018). However, it is a hazardous compound and has been shown to be present in industrial waste water and in fresh water where it comes from agricultural field run-off due to the degradation of organo-phosphorus pesticides (Wu et al., 2018). 4-NP is responsible for soil and water pollution because of its high level of toxicity. Due to this, the US Environmental Protection Agency (US EPA) has listed 4-NP as a priority pollutant. According to the US EPA the acceptable limit of 4-NP in potable water is

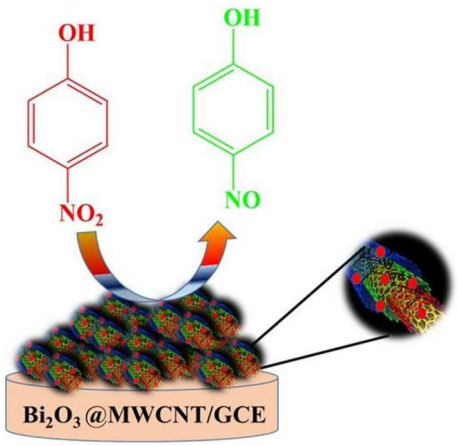

GRAPHICAL ABSTRACT | Electrochemical Determination of 4-Nitrophenol on Bi_2O_3@MWCNT Nano electrode.

only 60 ppb. Consuming even a small amount leads to acute effects in humans such as nausea, headache, drowsiness and cyanosis (Bose and Ramiah, 2017). It is even more dangerous as it can act as carcinogenic and mutagenic agent (Rajkumar et al., 2018). So there is an urgent need for the detection of 4-NP.

In the literature there are various methods employed for the determination of 4-NP *viz.* Belloli et al. (1999) determined 4-NP levels through a simple isocratic HPLC approach using seven columns, where the columns contained silica based C_{18} material. In this process a SiOH cartridge was used, which was treated with methyl chloride, dried with helium gas and stored at a low temperature. Sampling took 4 h. Guo et al. (2004) performed the separation and determination of phenol isomers by using capillary zone electrophoresis with methanol as an additive, it is an efficient method and about 10^5 theoretical plates per meter was achieved. Zhong et al. (2011) reported a method of detection in waste water, it is a 3-step process comprised of sample preparation, determination by GC-MS and subsequent analysis. Lin et al. (2013) proposed spectrophotometric detection, in which 4-NP was pre-concentrated with 1-hydroxy-2-naphthoic acid modified TiO_2, under optimum conditions more than 98% adsorption can be achieved by this method. Each method has certain limitations associated with it, such as the detection limit, sensitivity, selectivity, heavy instrumentation requirements, use of expensive gases, pretreatment etc. Moreover, the electrochemical method is a prominent technique for the detection of effluents like 4-NP as it is a rapid, cost effective, easy to operate, highly sensitive, and most importantly on-site measurement, that requires mild reaction conditions and has a low limit of detection. These factors make it a better alternative compared to the rest of the methods (Sun et al., 2012; Lin et al., 2013; Barman et al., 2017). Due to these factors, many electrochemical sensors have been reported for the determination of 4-NP. Chemically modified electrodes proved to be the best electrocatalysts as they increase the rate of reaction, provide a high surface area, have good stability and selectivity. A literature survey revealed that graphene based electrocatalysts (Li et al., 2012), metal and metal oxide electrocatalysts (Barman et al., 2017; Singh et al., 2017), metal-free electrocatalysts (Rajkumar et al., 2018), and their composites were all briefly studied as methods to determine 4-NP concentration.

There are several materials used as conductive substrates on which metal nanoparticles are anchored and grown including graphene (Chen et al., 2011), carbon nanotubes (Umar et al., 2016), Fullerene C_{60} (Li et al., 2019), graphitic carbon nitride (Liu et al., 2018; Hassannezhad et al., 2019) and conducting polymers like polyaniline (Wang G et al., 2018). Among these, carbon nanotubes have drawn attention since their inception in 1991, because of their unique properties including excellent electrical conductivity, large surface area, high electron density, exceptionally high mechanical and chemical stability, all of which makes them an ideal supporting material (Umar et al., 2016; Liu et al., 2018). Furthermore, the Ni based nanocomposite, $MgFe_2O_4$ NPs proved to be a good electrocatalyst for 4-nanoparticles (NPs) reduction (Baby et al., 2019; Mejri et al., 2019). Carbon nanotubes decorated with metals like Pt, Pd, Ag, monometallic-Au, and bimetallic-Au show excellent electrocatalytic activity toward nitrophenols (Liu et al., 2015; Umar et al., 2016; Sun et al., 2017; Dhanasekaran et al., 2019; Ding et al., 2019), but their low earth abundance and high cost inhibits their practical applicability. In order to address these issues researchers have proposed alternative approaches including replacing the precious metals with non-noble metals or producing metal free systems with high stability and cost effectiveness.

Literature shows that bismuth (Bi) and Bi_2O_3 films, nanoparticles and hybrids show excellent electrocatalytic activity toward 4-NP (Hutton et al., 2004; Lezi et al., 2014; Xia et al., 2014). This is because Bi and Bi_2O_3 electrocatalysts shows a high surface area, low band gap, and have good chemical and electrochemical properties. Additionally to this, Bi based systems have been shown to be1 good electrochemical sensors for heavy metals, biomolecules, drugs and for the electrocatalytic reduction of nitrates (Zhang et al., 2009; van der Horst et al., 2016; Sakthivel et al., 2019). These merits of Bi motivate researchers to use it for the electrochemical sensing of 4-NP. Bi proved to be a good alternative for precious metals as it is cost effective, sensitive, environmental friendly, versatile, and has a variety of uses (Hutton et al., 2004; Dortsiou and Kyriacou, 2009; Švancara et al., 2010; Wang W. et al., 2019). A Bi_2O_3 multiwalled carbon nanotube ($Bi2O_3$@MWCNT) composite might provide synergistic effects for the enhanced electrochemical detection of 4-NP. To date, and to the best of our knowledge, Bi_2O_3@MWCNTs has not been reported for 4-NP detection and quantification.

EXPERIMENTAL

Chemicals

MWCNTs 99.99%, Ethylene glycol (EG) 99.97%, Sulphuric acid 98%, Nitric acid 78%, Bismuth pentahydrate [$Bi(NO_3)_3$ $(H_2O)_5$], Acetone 99.99% and 4-NP (Para-nitrophenol) were purchased from Alfa-Aesar. All the chemicals were used as received for the synthesis of electrocatalysts and electrochemical studies were carried out in deionized water.

Characterization

X-ray diffraction (XRD) was carried out using a Rigaku Ultima IV fully automatic high-resolution X-ray diffractometer, with the X-ray generator operating at 40 kV and 40 mA at a step of 0.01(2θ) at room temperature. FTIR spectra were measured in the 4,000–400 cm^{-1} range on a Perkin-Elmer Spectrum-I spectrometer with samples prepared as KBr pellets. Raman spectroscopy was performed using a microscope with Raman optics (Seki Technetronic Corporation, Tokyo) with a 532 nm LASER.

Electrochemical Measurements

All electrochemical studies were performed on a CHI660C electrochemical works station (CH-Instrument) with a three electrode system. A glassy carbon (GC, 3 mm dia.) electrode was used as the working electrode to support the catalysts. A Pt foil and saturated SCE were used as the counter and reference electrodes, respectively. The GC electrode was polished with three different sizes of Al_2O_3 powder (1, 0.3, and 0.05 μm) followed by cleaning in an ultrasonic bath and finally rinsing with deionized water followed by ethanol. To prepare the working electrode, 0.5 mg as-synthesized catalyst was dispersed in a calculated amount (2–6 mL) of isopropyl alcohol under ultrasonic stirring for 40 min. An aliquot of the slurry was dropped onto the pre-polished GC electrode by using a micropipette and dried under an infrared lamp. The loading of catalyst on the electrode was calculated and used for normalization of the current.

Synthesis of Acid Functionalized Multiwalled Carbon Nanotubes (MWCNTs)

In a typical synthesis, 1 g of MWCNT powder was added to 120 mL nitrating mixture (30 mL HNO_3 and 90 mL H_2SO_4) in a round bottom flask which was placed in an ice bath under stirring for 30 min. Then mixture was then subjected to

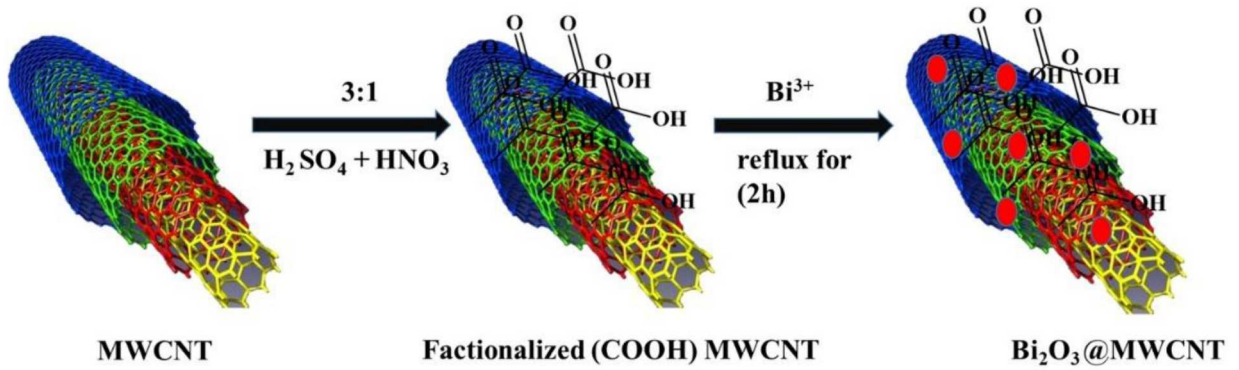

SCHEME 1 | Oxidative functionalization of MWNTs followed by decoration with Bi_2O_3 NPs.

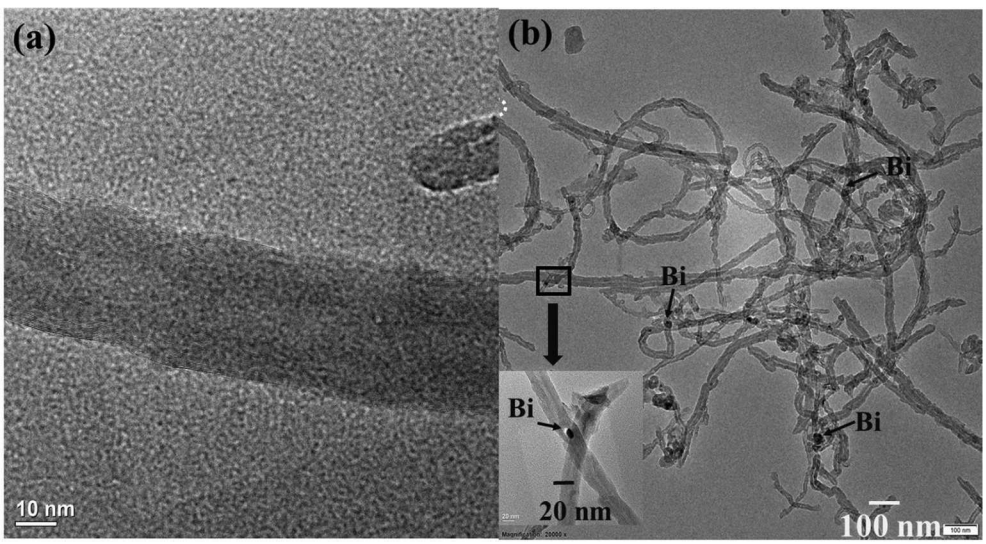

FIGURE 1 | (a) TEM image of MWCNTs showing that the average diameter is 10 nm, **(b)** TEM image of Bi_2O_3@MWCNTs showing that the average size of Bi_2O_3@MWCNTs is ∼20 nm.

ultrasonication at room temperature for 2 h. After sonication the dispersion was refluxed for 6 h, and a brown-gray paste was obtained after completion of the reaction (defined as diminished effervesence). After separating it *via* centrifugation, the brown-gray paste was re-dispersed in deionized (DI) water and subjected to ultrasonication for 3 h. After filtration the obtained solid material was washed with 1 M HCl, followed by an adequate amount of DI water until it turned into a black powdery material. These MWCNTs were used for further characterization and doping with bismuth.

Synthesis of Bi_2O_3 Decorated Multiwalled Carbon Nanotubes and Bi_2O_3 NPs

In a typical synthesis, 50 mL of ethylene glycol (EG) was heated at 110 °C for 30 min under constant stirring to remove dissolved oxygen and water molecules. This obtained anhydrous EG was used for further synthesis. Following this, 20 mg of acid functionalized MWCNTs were added to 50 mL anhydrous EG and dispersed by sonication for 3 h. On complete dispersion of the MWCNTs, bismuth nitrate (0.02 gm in 50 mL EG) was added dropwise under constant stirring and stirring continued for 3 h. Then this reaction mixture was refluxed for 6 h. The resultant product was cooled to RT then filtered and washed with acetone. The obtained black colored catalyst was dried in the oven at 60°C for 2 h which results in Bi_2O_3@MWCNTs

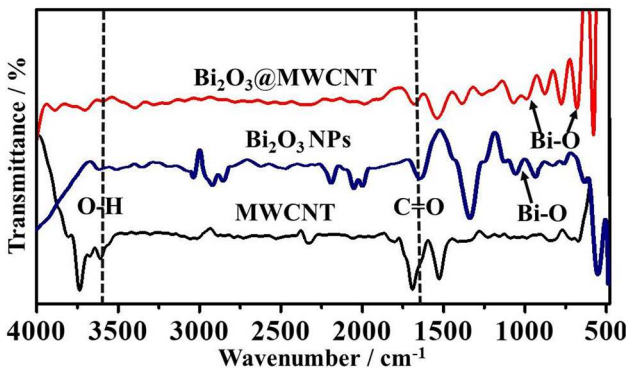

FIGURE 2 | Superimposed FTIR spectra of MWCNTs, Bi_2O_3 NPs and Bi_2O_3@MWCNTs. Acid functionalization followed by Bi_2O_3 decoration is confirmed by the appearance of additional signals corresponding to Bi-O.

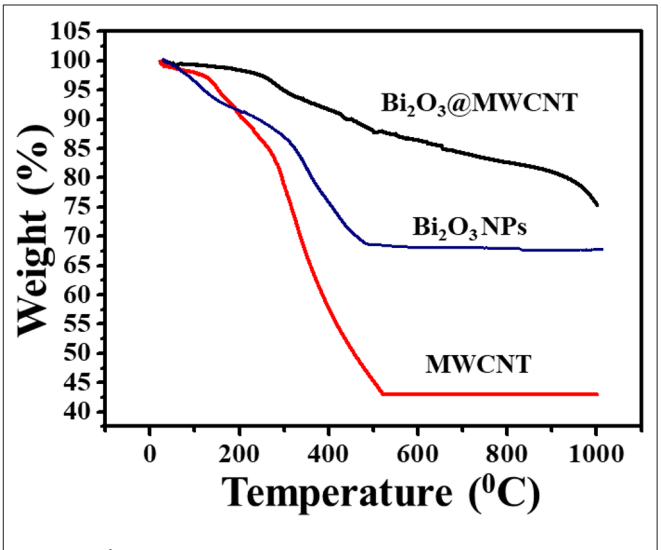

FIGURE 4 | Superimposed TGA profiles for MWCNTs, Bi_2O_3 NPs and the Bi_2O_3@MWCNTs nanocomposite in an air atmosphere.

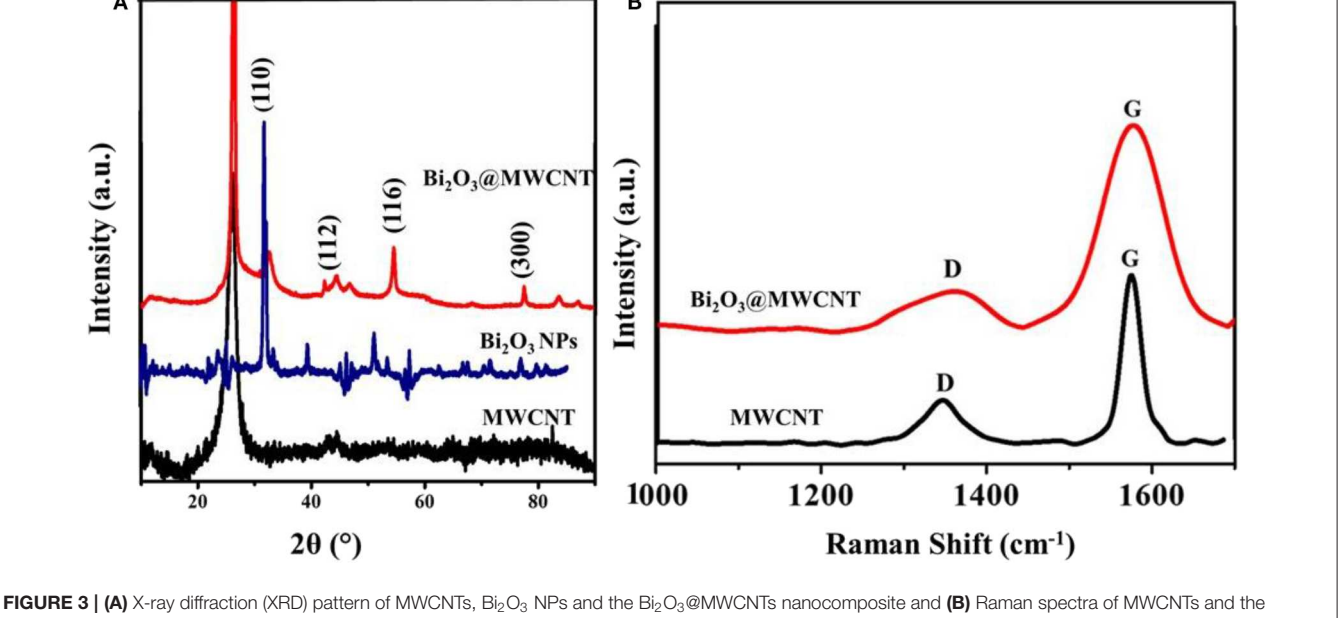

FIGURE 3 | (A) X-ray diffraction (XRD) pattern of MWCNTs, Bi_2O_3 NPs and the Bi_2O_3@MWCNTs nanocomposite and **(B)** Raman spectra of MWCNTs and the Bi_2O_3@MWCNTs nanocomposite.

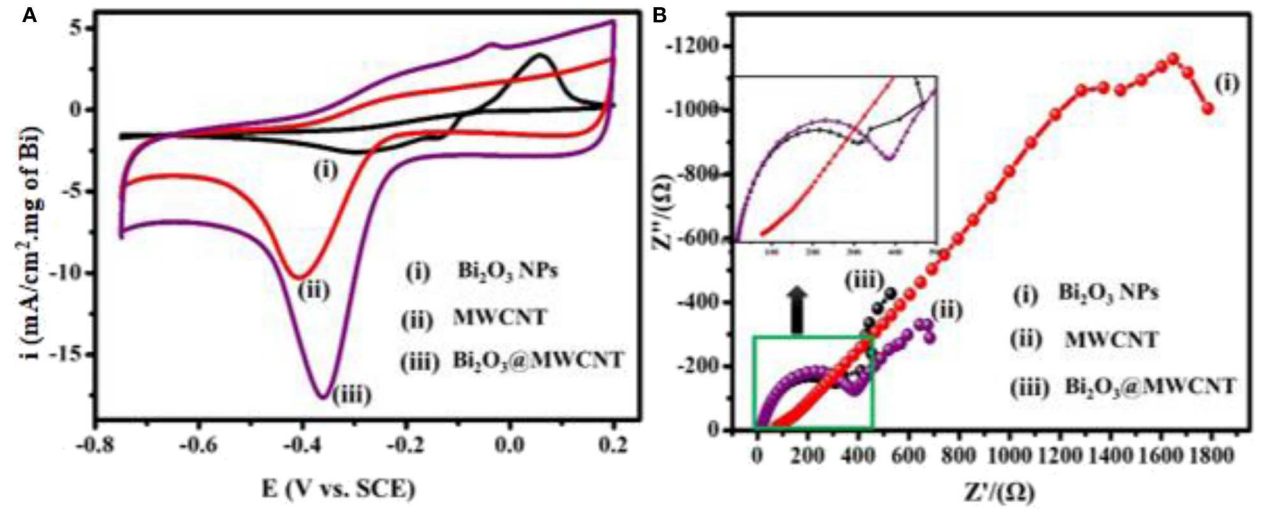

FIGURE 5 | (A) CV of (i) Bi_2O_3 NPs (ii) MWCNTs (iii) Bi_2O_3@MWCNTs in the presence of 4 mM 4-NP in 0.5M H_2SO_4 at 50 mV/s, **(B)** Nyquist plots for (i) Bi_2O_3 NPs (ii) MWCNTs (iii) Bi_2O_3@MWCNTs in the presence of 4 mM 4-NP in 0.5 M H_2SO_4 at 50 mV/s (current density is normalized with loading of Bi_2O_3 NPs in Bi_2O_3@ MWNTs calculated from TG analysis).

TABLE 1 | Comparative data of onset potential and peak current density of electrocatalysts.

Sr.No.	Electrocatalyst	Onset Potential (V vs. SCE)	Current density i (mA/cm^2)
1	Bi_2O_3 NPs	−0.19	2.6
2	MWCNTs	−0.24	10.0
3	Bi_2O_3@MWCNTs	−0.17	17.62

nanocomposite formation and is demonstrated schematically in **Scheme 1**. Similarly, Bi_2O_3 NPs were synthesized without the addition of MWCNTs.

RESULTS AND DISCUSSION

The morphological and structural features of electrocatalysts were identified by TEM and are shown in **Figure 1a**. The TEM image of the MWCNTs shows the average diameter is ∼10 nm. Moreover, **Figure 1b** shows the TEM for Bi_2O_3@MWCNTs. MWCNTs were found to provide a large surface area for crystalline Bi NPs with spherical shape. Further, the superimposed FTIR spectrum of MWCNTs, Bi_2O_3 NPs and Bi_2O_3@MWCNTs is displayed in **Figure 2** and it clearly shows bands appearing at 1,500, 1,700, and 3,600 cm^{-1} which correspond to the stretching frequencies of oxygen in C=O, aromatic C=C and O-H, respectively, all of which are functional groups present on MWCNTs.

Bi_2O_3@MWCNTs clearly indicates that the peak around 600 cm^{-1} and 1,000 cm^{-1} corresponds to Bi-O stretching frequencies (Chipeture et al., 2019). The XRD (crystal structure) images of MWCNTs and Bi_2O_3@MWCNTs is displayed in **Figure 3A** and shows sharp signals for Bi_2O_3 NPs and MWCNTs in the 2θ of range 10 to 90°. The characteristic diffraction patterns (002) and (101) correspond to the MWCNTs, which closely agree with reported functionalized MWCNTs systems. Moreover, Bi_2O_3 has an α-metastable crystal structure that was confirmed by corresponding peaks observed at the (110), (116), and (300) planes. Raman spectra for MWCNTs and the Bi_2O_3@MWCNTs composite are shown in **Figure 3B**. In case of MWCNTs a signal appeared corresponding to the D band at 1,345 cm^{-1} and the G band at 1,570 cm^{-1} and their associated intensity ratio (i.e., I_D/I_G) ratio is 0.32. For Bi_2O_3@MWCNTs the calculated intensity ratio, I_D/I_G, is 0.88. The increase of I_D/I_G by more than double confirms an increase in the disorder in MWCNTs after decoration with Bi_2O_3 NPs. It is in good agreement with previous reports (Thi Mai Hoa, 2018).

Thermogravimetric analysis deals with weight loss during decomposition as a function of temperature, in the range of 0–1,000°C. In case of MWCNTs the degree of functionalization, i.e., the extent to which carboxylic groups were grafted onto MWCNTs, was confirmed by TGA. **Figure 4** shows the superimposed TGA curves for MWCNTs, Bi_2O_3 NPs and Bi_2O_3@MWCNTs. In the case of MWCNTs (red line) a two-step decomposition has been observed, in the first step, which ranges from 100 to 300°C, ∼ 23% of weight was lost due to the loss of water molecules and other volatile species. In the second stage, ranging between 300 and 520°C, rapid weight loss was observed to give an overall weight loss of 58%, this could be due to functional groups like –COOH and is in good agreement with the literature (Thi Mai Hoa, 2018). In the case of Bi_2O_3 NPs (blue line) a two-step weight loss is observed. The first step between 70 and 270°C corresponds to 13% weight loss due to the elimination of water and other impurities. While in the second step, after 270°C, an overall 33 % weight loss is observed. This is due to the low melting point of Bi (271°C) and the removal of capping molecules. When compared to MWCNTs & Bi_2O_3 NPs,

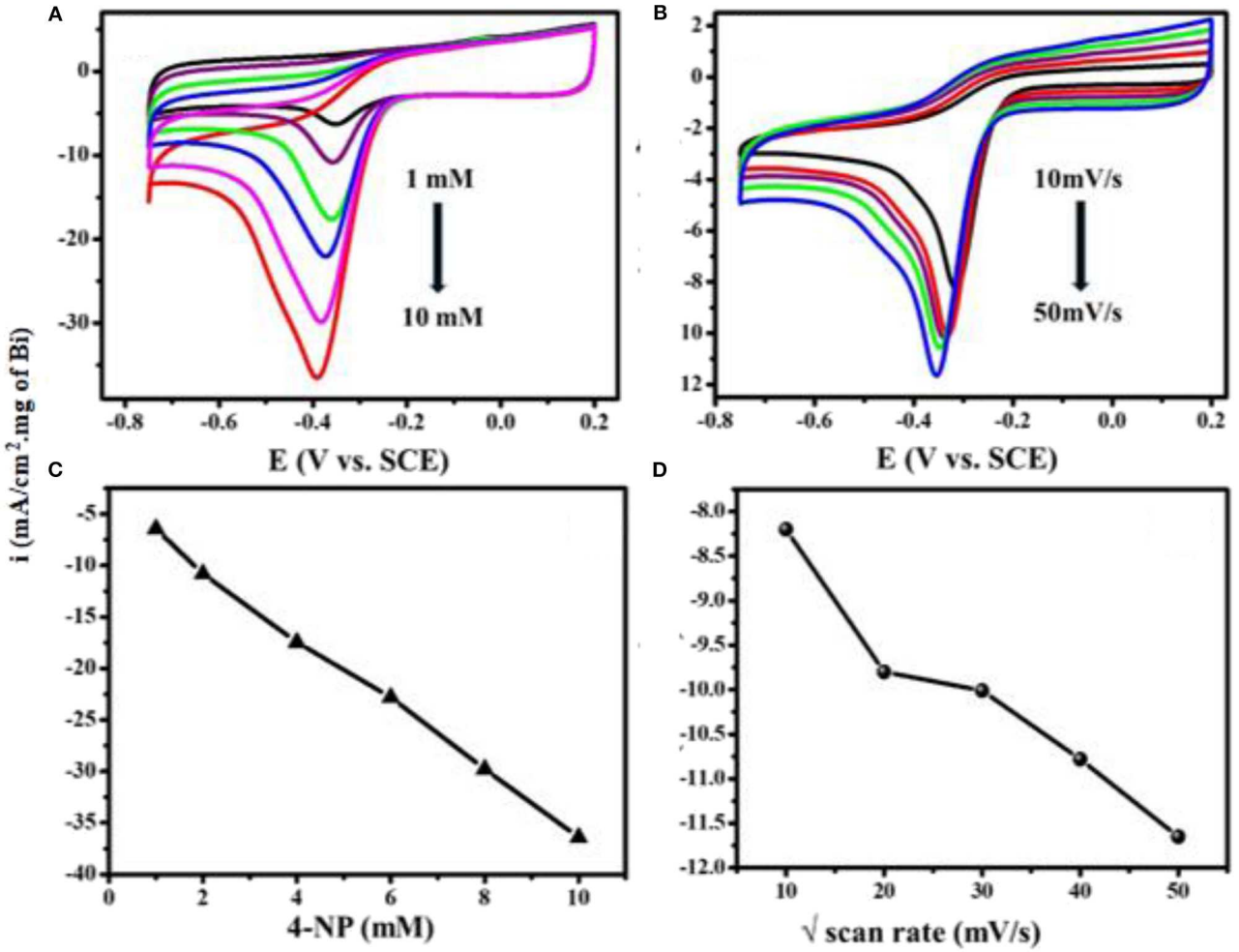

FIGURE 6 | Superimposed CV curves of Bi_2O_3@MWCNTs in 0.5 M H_2SO_4 **(A)** at different concentrations from 1 mM to 10 mM of 4-NP at a scan rate of 50 mV/s **(B)** at different scan rates (10–50 mV/s) for 4 mM of 4-NP. **(C)** shows the linear fit for peak current density vs. concentration and **(D)** linear fit peak for the scan rate of 4-NP on Bi_2O_3@MWCNTs (current density is normalized with loading of Bi_2O_3 NPs in Bi_2O_3@ MWNTs calculated from TG analysis).

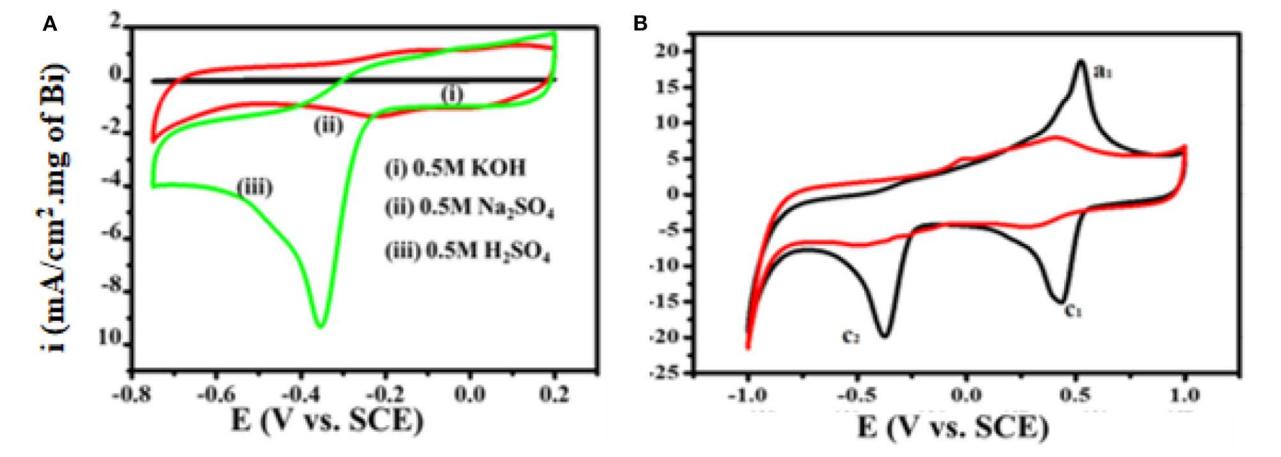

FIGURE 7 | (A) Superimposed CV curves for 4-NP sensing in different media **(B)** CV obtained at Bi_2O_3@MWCNTs without 4-NP (red line) and Bi_2O_3@MWCNTs with 4-NP (black line) in 0.5 M H_2SO_4 with a potential window of −1.0 to 1.0, at scan rate 50 mV/s.

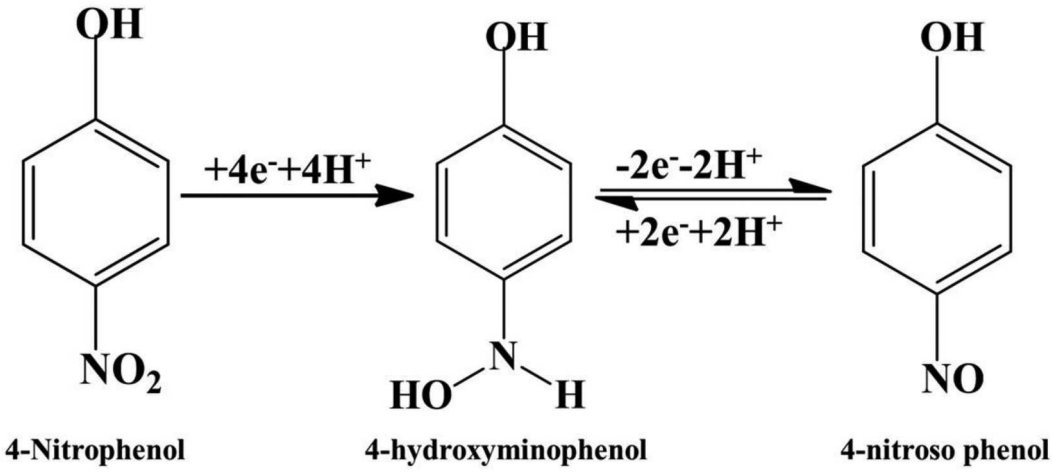

FIGURE 8 | Mechanism of 4-Nitrophenol reduction on Bi_2O_3@MWCNTs.

the Bi@MWCNTs nanocomposite (black line) shows much more thermal stability. It shows a rapid decomposition after 271°C which is attributed to the low melting point of bismuth.

Electrochemical Studies Toward 4-Nitrophenol as an Organic Pollutant

The electrochemical behavior of as-synthesized electrocatalytic systems was investigated by using cyclic voltammetry (CV) in 0.5 M H_2SO_4 as a supporting electrolyte. **Figure 5A** shows the CV response of Bi_2O_3 NPs, MWCNTs, and Bi_2O_3@MWCNTs in the presence of 4-NP (4 mM) in 0.5 M H_2SO_4 at a scan rate of 50 mV/s. It has been observed that Bi_2O_3 NPs show the smallest reduction peak but MWCNTs shows a slightly higher reduction peak. In the case of Bi_2O_3@MWCNTs a significant increase in reduction peak was observed which confirms the synergistic effect of Bi_2O_3 and MWCNTs, i.e., due to increases in the electron density of Bi and the higher accessible surface of MWCNTs toward 4-NP sensing.

Electrochemical Impedance Spectroscopy (EIS) is an efficient tool which provides insights about the interfacial picture during electron transfer at interfaces (Wu et al., 2018) during the reductive sensing of 4-NP. In EIS studies the diameter of a semicircle is directly proportional to electron transfer resistance which governs the electron transfer kinetics (He et al., 2019). **Figure 5B** shows Nyquist plots for Bi_2O_3 NPs, MWCNTs and Bi_2O_3@MWCNTs in 0.5 M H_2SO_4. The larger semi-circle observed for Bi_2O_3 NPs and MWCNTs reflects a higher electron transfer resistance. On the contrary Bi_2O_3@MWCNTs (309 Ω) shows a small semi-circle which reflects a lower electron transfer resistance which results in higher electrocatalytic activity toward 4-NP reduction compared to Bi_2O_3 NPs (1,000 Ω) and MWCNTs (400 Ω). These result are in good agreement with cyclic voltammetry results. **Table 1** shows comparative data of the onset potential and peak current density of electrocatalysts, it can be seen that the Bi_2O_3@MWCNTs nanocomposite has a lower negative onset potential and higher peak current density as compared to Bi_2O_3 NPs and MWCNTs, respectively.

Figure 6A shows superimposed CV curves for different concentrations of 4-NP on Bi_2O_3@MWCNTs in 0.5 M H_2SO_4 at a scan rate of 50 mV/s. The reduction peak current increases linearly with concentration (1, 2, 4, 6, 8, 10 mM) which means Bi_2O_3@MWCNTs shows efficient electrochemical sensing toward 4-NP. **Figure 6B** shows scan rate dependent studies on the reduction peak current of Bi_2O_3@MWCNTs, in 0.5 M H_2SO_4 at a concentration of 4 mM. The variations in their linearity with current density and positive shift in potential could be due to diffusion controlled 4-NP reduction processes as shown in **Figures 6C,D**.

Figure 7A shows 4-NP electrochemical sensing by the Bi_2O_3@MWCNTs nanocomposite in acidic, basic and neutral media. As electroreduction of 4-NP is a proton involving step, the pH of the supporting electrolyte affects the electrochemical processes. From **Figure 7A** it is evident that a distinct reduction peak is observed in the case of an acidic medium as compared to neutral and basic media. This is due to the fact that protons replaced the 4-NP present on electrode surface, as the pH of the medium is increased nitrogen anions prevent the approach of 4-NP to the electrode surface (Wu et al., 2018). The mechanism has been proposed for the electrochemical reduction of 4-NP on Bi_2O_3@MWCNTs on the basis of CV is shown in **Figure 7B.** There is not an appreciable peak observed in the absence of 4-NP (red line) while in the presence (black line) of 4-NP the redox couple is observed at $Ea_1 = 0.52$ and $Ec_1 = 0.43$ and the reduction peak is at $Ec_2 = -0.37$ which confirms the reduction of 4-NPs.

The C_2 peak symbolizes the formation of 4-hydroxylaminophenol which is an irreversible reaction while the redox couple is due to the interconversion of 4-hydroxylnitrophenol and 4-nitrosophenol (Rajkumar et al., 2018; He et al., 2019).

TABLE 2 | Comparison of 4-nitrophenol determination with Bi_2O_3@MWCNTs as with other electrocatalysts reported in literature.

Sr. No.	Electrocatalyst	Technique	Linear range	LOD (μM)	References
1	S-GCN/SPCE	i-t	0.05–90 μm	-	Rajkumar et al., 2018
2	β -CD/SiC/GCE	i-t	5–150 μM	-	Wu et al., 2018
3	Cu-Curcumin/GCE	DPV	0.1–1,030 μM	-	Bose and Ramiah, 2017
4	Ag NPs –decorated TA@Fe_3O_4/GCE	DPV	0.1–680 μM	-	Sangili et al., 2018
5	Au@MWCNTs/GCE	i-t	1×10^{-8} to 5×10^{-4} M	-	Al-Kahtani et al., 2018
6	SWCNT/GCE	i-t	1×10^{-8} to 5×10^{-6} M	-	Yang, 2004
7	FeOx/TiO_2@mC/GCE	CV	5–310μM	0.183	Wang M. et al., 2019
8	α- MnO_2/MWCNTs	CV	30–475 μM	0.186	Anbumannan et al., 2019
9	2D $ZnCo_2O_4$ Nanosheets	DPV	1–4,000 μM	0.3	Zhang et al., 2018
10	DTD/AgNPs/CPE	CV	1–100	0.25	Rounaghi et al., 2011
11	RGO/Fe_3O_4NPs/GCE	DPV	0.2–10 μM	0.26	Cheng et al., 2017
		SWV	20–100 μM	0.86	
12	Cu_2O Sheets	CV	0.006-2.72 μM	0.5	Veeramani et al., 2016
13	GNFs/GCE	CV	1–6000	0.7	Wang et al., 2014
14	Bi_2O_3@MWCNTs	CV	1-10 mM	0.10	This work

The electrochemical mechanism is given in **Figure 8**.

Limit of Detection (4-NP)

The limit of detection is an important parameter for analytical method validation. **Figure 6A** depicts cyclic voltammetric response for different concentrations of 4-NP vs. peak current densities. Accordingly,

$$LOD = 3(S/M) \quad (1)$$

Where, S, Standard deviation; M, Slope point.

The LOD is calculated by using equation 1 and the LOD was calculated to be 0.1 μM (Mulik et al., 2018). Finally it is found that a smaller LOD confirms the actual apparent concentration of the 4-NP reduction reaction. In addition to this, our work has been compared with the reported literature. **Table 2** summarizes reported electrocatalytic systems with their linearity range and LOD upon comparison proposed Bi_2O_3@MWCNTs system for 4-NP reduction (Mulik et al., 2018).

CONCLUSION

The Bi_2O_3@MWCNTs electrocatalyst was synthesized by using a simple chemical reduction method. As-synthesized nanomaterials MWCNTs, Bi_2O_3 and Bi_2O_3@MWCNTs NPs have been well-characterized by FTIR which confirms the Bi-O bonding in Bi_2O_3@MWCNT. XRD shows the Bi_2O_3@MWCNTs was in an α-metastable crystal structure. Raman spectra show the I_D/I_G ratio increases in Bi_2O_3@MWCNTs as compared with MWCNTs, and it is confirmed that there are more sp^2 C, TEM analysis confirms the average size is ∼10 nm. The improved monometallic Bi supporting MWCNTs provides a higher surface area which results in a significant increase in the electrocatalytic activity with an onset potential of −0.17 V toward electrochemical 4-NP reduction. As compared to reported systems, this is a cost effective and highly efficient system for the determination of 4-NP.

DATA AVAILABILITY STATEMENT

The datasets generated for this study are available on request to the corresponding author.

AUTHOR CONTRIBUTIONS

RD has conducted all experiments and written the manuscript. AM and BM have helped to interpret the characterization data, whereas BS has invigilated the whole project with his expert advice and fruitful suggestions.

FUNDING

This study was financially supported by DST-SERB, New Delhi (SERB/F/7490/2016-17) and DAE-BRNS, Mumbai research project No (F. No. 34/20/06/2014-BRNS/21gs), DST-SERB, New Delhi. (SERB/F/7490/2016-17) I RPD especially thankful to DST-SERB, New Delhi and Dr. Babasaheb Ambedkar Marathwada University, Aurangabad (MS) (STAT/VI/RG/DEPT/2019-20/327-28 for 2019-2020) for financial assistance. Department of Chemistry, Dr. Babasaheb Ambedkar Marathwada University, Aurangabad for providing necessary research laboratory facilities.

REFERENCES

Al-Kahtani, A. A., Almuqati, T., Alhokbany, N., Ahamad, T., Naushad, M., and Alshehri, S. M. (2018). A clean approach for the reduction of hazardous 4-nitrophenol using gold nanoparticles decorated multiwalled carbon nanotubes. *J. Clean. Produc.* 191, 429–435. doi: 10.1016/j.jclepro.2018.04.197

Anbumannan, V., Dinesh, M., Rajendrakumar, R. T., and Suresh, K. (2019). Hierarchical α-MnO_2 wrapped MWCNTs sensor for low level detection of p-nitrophenol in water. *Ceram. Int.* 45, 23097–23103. doi: 10.1016/j.ceramint.2019.08.002

Baby, J., Sriram, B., Wang, S., and George, M. (2019). Effect of various deep eutectic solvents on the sustainable synthesis of MgFe2O4 nanoparticles for simultaneous electrochemical determination of nitrofurantoin and 4-nitrophenol. *ACS Sustainable Chem. Eng.* 8, 1479–1486. doi: 10.1021/acssuschemeng.9b05755

Barman, K., Changmai, B., and Jasimuddin, S. K. (2017). Electrochemical detection of para-nitrophenol using copper metal nanoparticles modified gold electrode. *Electroanalysis 29,* 2780–2787. doi: 10.1002/elan.201700430

Belloli, R., Barletta, B., Bolzacchini, E., Meinardi, S., Orlandi, M., and Rindone, B. (1999). Determination of toxic nitrophenols in the atmosphere by high-performance liquid chromatography. *J. Chromatogr. A* 846, 277–281. doi: 10.1016/s0021-9673(99)00030-8

Bose, D., and Ramiah, S. (2017). Electrochemical synthesis of nanostructured copper-curcumin complex and its electrocatalytic application towards reduction of 4-nitrophenol. *Sens. Actuators B Chem.* 253, 502–512. doi: 10.1016/j.snb.2017.06.149

Chen, X., Wu, G., Chen, J., Chen, X., Xie, Z., and Wang, X. (2011). Synthesis of "Clean" and well-dispersive Pd nanoparticles with excellent electrocatalytic property on graphene oxide. *J. Am. Chem. Soc.* 133, 3693–3695. doi: 10.1021/ja110313d

Cheng, Y., Li, Y., Li, D., Zhang, B., Hao, R., and Sang, S. (2017). A Sensor for Detection of 4-nitrophenol Based on a Glassy Carbon Electrode Modified with a Reduced Graphene Oxide/Fe3O4 Nanoparticle Composite. *Int. J. Electrochem. Sci.*, 7754–7764. doi: 10.20964/2017.08.08

Chipeture, A. T., Apath, D., Moyo, M., and Shumba, M. (2019). Multiwalled carbon nanotubes decorated with bismuth (III) oxide for electrochemical detection of an antipyretic and analgesic drug paracetamol in biological samples. *J. Anal. Sci. Technol.* 10:22. doi: 10.1186/s40543-019-0181-5

Dhanasekaran, T., Manigandan, R., Padmanaban, A., Suresh, R., Giribabu, K., and Narayanan, V. (2019). Fabrication of Ag@Co-Al layered double hydroxides reinforced poly(o-phenylenediamine) nanohybrid for efficient electrochemical detection of 4-nitrophenol, 2,4-dinitrophenol and uric acid at nano molar level. *Sci. Rep.* 9:13250. doi: 10.1038/s41598-019-49595-y

Ding, Q. K., Zewen, C., Liping, L., Mengshi, Lin, H., and Yang, D. (2019). Conversion of waste eggshell into difunctional Au/$CaCO_3$ nanocomposite for 4-nitrophenol electrochemical detection and catalytic reduction. *Appl. Surf. Sci.* 510:145526. doi: 10.1016/j.apsusc.2020.145526

Dortsiou, M., and Kyriacou, G. (2009). Electrochemical reduction of nitrate on bismuth cathodes. *J. Electroanal. Chem.* 630, 69–74. doi: 10.1016/j.jelechem.2009.02.019

Guo, X., Wang, Z., and Zhou, S. (2004). The separation and determination of nitrophenol isomers by high performance capillary zone electrophoresis. *Talanta* 64, 135–139. doi: 10.1016/j.talanta.2004.01.020

Hassannezhad, M., Hosseini, M., Ganjali, M. R., and Arvand, M. (2019). Graphitic carbon nitride (g-C_3N_4/Fe_3O_4) nanocomposite: an efficient electrode material for electrochemical determination of tramadol in human biological fluids. *Anal. Methods* 11, 2064–2071. doi: 10.1039/c9ay00146h

He, Q., Tian, Y., Wu, Y., Liu, J., Li, G., Deng, P., et al. (2019). Facile and ultrasensitive determination of 4-nitrophenol based on acetylene black paste and graphene hybrid electrode. *Nanomaterials* 9, 1–16. doi: 10.3390/nano.9030429

Hutton, E. A., Ogorevc, B., and Smyth, M. R. (2004). Cathodic electrochemical detection of nitrophenols at a bismuth film electrode for use in flow analysis. *Electroanalysis* 16, 1616–1621. doi: 10.1002/elan.200402979

Lezi, N., Economou, A., Barek, J., and Prodromidis, M. (2014). Screen-printed disposable sensors modified with bismuth precursors for rapid voltammetric determination of 3 ecotoxic nitrophenols. *Electroanalysis* 26, 766–775. doi: 10.1002/elan.201400001

Li, J., Kuang, D., Feng, Y., Zhang, F., Xu, Z., and Liu, M. (2012). A graphene oxide-based electrochemical sensor for sensitive determination of 4-nitrophenol. *J. Hazard Mater.* 201–202, 250–259. doi: 10.1016/j.jhazmat.2011.11.076

Li, Z., Zhang, Y., Zhua, R., Wena, G., Dong, C., and Li, H. W. (2019). Self-assembled palladium nanoflowers supported on fullerene Electrochemical catalytic performance for the reduction of 4-nitrophenol. *Electrochem. Commun.* 104:106484. doi: 10.1016/j.elecom.2019.106484

Lin, X., Chen, Y., and Li, S. (2013). Spectrophotometric determination of trace *p*-nitrophenol enriched by 1-hydroxy-2-naphthoic acid-modified nanometer TiO_2 in water. *Anal. Methods* 5, 6480–6485. doi: 10.1039/C3AY41467A

Liu, C. H., Liu, J., Zhou, Y. Y., Cai, X. L., Lu, Y., Gao, X., et al. (2015). Small and uniform Pd monometallic/bimetallic nanoparticles decorated on multi-walled carbon nanotubes for efficient reduction of 4-nitrophenol. *Carbon* 94, 295–300. doi: 10.1016/j.carbon.2015.07.003

Liu, Y., Zhang, J., Cheng, Y., and Jiang, S. P. (2018). Effect of carbon nanotubes on direct electron transfer and electrocatalytic activity of immobilized glucose oxidase. *ACS Omega* 3, 667–676. doi: 10.1021/acsomega.7b01633

Mejri, A., Mars, A., Elfil, H., and Hamzaoui, A. H. (2019). Reduced graphene oxide nanosheets modified with nickel disulphide and curcumin nanoparticles for non-enzymatic electrochemical sensing of methyl parathion and 4-nitrophenol. *Microchimica Acta*. 186:704. doi: 10.1007/s00604-019-3853-3

Mulik, B., Dhumal, S., Harale, R., Kharat, K., and Sathe, B. (2018). Electrochemical studies of anti-hiv drug emtricitabine: oxidative determination and improved antimicrobial activity. *Chem. Electrochem.* 5, 3926–3931. doi: 10.1002/celc.201801228

Rajkumar, C., Veerakumar, P., Chen, S., Thirumalraj, B., and Lin, K. C., (2018). Ultrathin sulphur-doped graphitic carbon nitride nano sheets as metal-free catalyst for electrochemical sensing and catalytic removal of 4-nitrophenol. *ACS Sus. Chem. Eng.* 6, 16021–16031. doi: 10.1021/acssuschemeng.8b02041

Rounaghi, G., kakhki, R. M., and Azizi-toupkanloo, H. (2011). Voltammetric determination of 4-nitrophenol using a modified carbon paste electrode based on a new synthetic crown ether/silver nanoparticles. *Mater. Sci. Eng. C* 32, 172–177. doi: 10.1016/j.msec.2011.10.014

Sakthivel, R., Kubendhiran, S., and Chen, S. M. (2019). Facile one-pot sonochemical synthesis of ni doped bismuth sulfide for the electrochemical determination of promethazine hydrochloride. *Ultrason. Sonochem.* 54:68–78. doi: 10.1016/j.ultsonch.2019.02.013

Sangili, A., Annalakshmi, M., Chen, S. M., Balasubramanian, P., and Sundrarajan, M. (2018). Synthesis of silver nanoparticles decorated on core-shell structured tannic acid coated iron oxide nanospheres for excellent electrochemical detection and efficient catalytic reduction of hazardous 4-nitrophenol. *Compos Part B-Eng.* 162, 33–42. doi: 10.1016/j.compositesb.2018.10.084

Singh, S., Kumar, N., Kumar, J., Agrawal, A., and Mizaikoff, B. (2017). Electrochemical sensing and remediation of 4-nitrophenol using bio-synthesized copper oxide nanoparticles. *Chem. Eng. J.* 313, 283–292. doi: 10.1016/j.cej.2016.12.049

Sun, Z., Song, G., Du, R., and Hu, X. (2017). Modification of a Pd-loaded electrode with a carbon nanotubes–polypyrrole interlayer and its dechlorination performance for 2, 3-dichlorophenol. *RSC Adv.* 7, 22054–22062. doi: 10.1039/C7RA02515G

Sun, Z., Wei, X., Hu, X., Wang, K., and Shen, H. (2012). Electrocatalytic dechlorination of 2,4-dichlorophenol in aqueous solution on palladium loaded meshed titanium electrode modified with polymeric pyrrole and surfactant. *Colloids Surf. A Physicochem.* 414, 314–319. doi: 10.1016/j.colsurfa.2012.08.035

Švancara, I., Prior C, Hočevar, S. B., and Wang, J. A. (2010). Decade with bismuth-based electrodes in electroanalysis. *Electroanalysis* 22, 1405–1420. doi: 10.1002/elan.200970017

Thi Mai Hoa, L. (2018) Characterization of multi-walled carbon nanotubes functionalized by a mixture of HNO_3/H2SO_4. *Diam. Relat. Mater.* 89, 43–51. doi: 10.1016/j.diamond.2018.08.008

Umar, A., Kim, S., Kumar, R., Algarni, H., and Al-Assiri, M. S. (2016). Platinum nanoparticles decorated carbon nanotubes for highly sensitive 2-nitrophenol chemical sensor. *Ceramics Int.* 42, 9257–9263. doi: 10.1016/j.ceramint.2016.03.032

van der Horst, C., Silwana, B., Iwuoha, E., Gil, E., and Somerset, V. (2016) Improved detection of ascorbic acid with a bismuth-silver nanosensor. *Food Anal. Methods* 9, 2560–2566. doi: 10.1007/s12161-016-0444-3

Veerakumar, P., Chen, S. M., Madhu, R., Veeramani, V., Hung, C. T., and Liu, S. B. (2015). Nickel nanoparticle-decorated porous carbons for highly active catalytic reduction of organic dyes and sensitive detection of Hg(II) ions. *ACS Appl. Mater. Interfaces* 7, 24810–24821. doi: 10.1021/acsami.5b07900

Veeramani, V., Sivakumar, M., Chen, S.-M., Madhu, R., Dai, Z.-C., and Miyamoto, N. (2016). A facile electrochemical synthesis strategy for Cu_2O (cubes, sheets and flowers) microstructured materials for sensitive detection of 4-nitrophenol. *Anal. Method* 8, 5906–5910. doi: 10.1039/c6ay01388k

Wang G, Morrin, A., Li, M., Liu, N., and Luo, X. (2018). Nanomaterial-doped conducting polymers for electrochemical sensors and biosensors. *J. Mater. Chem. B* 6, 4173–4190. doi: 10.1039/c8tb00817e

Wang, M., Liu, Y., Yang, L., Tian, K., He, L., Zhang, Z., Fang, S. (2019). Bimetallic metal–organic framework derived FeO /TiO2 embedded in mesoporous carbon nanocomposite for the sensitive electrochemical detection of 4-nitrophenol. *Sens. Actu. B Chemical*. 281, 1063–1072. doi: 10.1016/j.snb.2018.11.083

Wang, P., Xiao, J., Guo, M., Xia, Y., Li, Z., Jiang, X., and Huang, W. (2014). Voltammetric Determination of 4-Nitrophenol at Graphite Nanoflakes Modified Glassy Carbon Electrode. *J. Electrochem. Soc.* 162, H72–H78. doi: 10.1149/2.0991501jes

Wang, W., Xiao, Y., Li, X., Cheng, Q., and Wang, G. (2019). Bismuth oxide self-standing anodes with concomitant carbon dots welded graphene layer for enhanced performance supercapacitor-battery hybrid devices. *Chem. Eng. J.* 371, 327–336. doi: 10.1016/j.cej.2019.04.048

Wu, S., Fan, S., Tan, S., Wang, J., and Li, C. (2018). A new strategy for the sensitive electrochemical determination of nitrophenol isomers using β-cyclodextrin derivative-functionalized siliconcarbide. *RSC Adv*. 8, 775–784. doi: 10.1039/c7ra12715d

Xia, F., Xu, X., Li, X., Zhang, L., Zhang, L., Qiu, H., et al. (2014). Preparation of bismuth nanoparticles in aqueous solution and its catalytic performance for the reduction of 4-nitrophenol. *Ind. Eng. Chem. Res.* 53, 10576–10582. doi: 10.1021/ie501142a

Yang, C. (2004) Electrochemical determination of 4-nitrophenol using a single-wall carbon nanotube film-coated glassy carbon electrode. *Microchimica Acta* 148, 87–92. doi: 10.1007/s00604-004-0240-4

Zhang, J., Cui, S., Ding, Y., Yang, X., Guo, K., and Zhao, J. (2018). Two-dimensional mesoporous $ZnCo_2O_4$ nanosheets as a novel electrocatalyst for detection of o-nitrophenol and p-nitrophenol. *Biosens. Bioelectron.* 112, 177–185. doi: 10.1016/j.bios.2018.03.021

Zhang, Z., Yu, K., Bai, D., and Zhu, Z. (2009). Synthesis and electrochemical sensing toward heavy metals of bunch-like bismuth nanostructures. *Nanoscale Res. Lett*. 5, 398–402. doi: 10.1007/s11671-009-9495-3

Zhong, W. J., Wang, D. H., Xu, X. W., Wang, B. Y., Luo, Q., Senthilkumaran, S., et al. (2011). A gas chromatography/mass spectrometry method for the simultaneous analysis of 50 phenols in wastewater using deconvolution technology. *Chinese Sci. Bull.* 56, 275–284. doi: 10.1007/s11434-010-4266

Conflict of Interest: The authors declare that the research was conducted in the absence of any commercial or financial relationships that could be construed as a potential conflict of interest.